Available online at www.sciencedirect.com
ScienceDirect
Ceramics International 36 (2010) 2129–2135
CERAMICS INTERNATIONAL
www.elsevier.com/locate/ceramint

Wear mechanisms of TiN–TiB_2 ceramic in sliding against alumina from room temperature to 700 °C

Zhen-Lin Yang, Jia-Hu Ouyang *, Zhan-Guo Liu, Xue-Song Liang

Institute for Advanced Ceramics, Department of Materials Science, Harbin Institute of Technology, No. 92, West Da-Zhi Street, Harbin 150001, China

Received 8 March 2010; received in revised form 19 March 2010; accepted 2 May 2010
Available online 18 June 2010

Abstract

TiN–TiB_2 ceramic was prepared by the reactive hot-pressing method using titanium and BN powders as raw materials. The friction and wear properties of TiN–TiB_2 ceramic were evaluated in sliding against alumina ball from room temperature to 700 °C in air. The TiN–TiB_2 ceramic has a relative density of 98.6%, a flexural strength of 731.9 MPa and a fracture toughness of 8.5 MPa $m^{1/2}$ at room temperature. The TiN–TiB_2 ceramic exhibits a distinct decrease in friction coefficient at 700 °C as contrasted with the friction data obtained at room temperature and 400 °C. Wear mechanisms of TiN–TiB_2 ceramic depend mainly upon testing temperature at identical applied loads. Lubricious oxidized products caused by thermal oxidation provide excellent lubrication effects and greatly reduce the friction coefficient of TiN–TiB_2 ceramic at 700 °C. However, abrasive wear and tribo-oxidation are the dominant wear mechanisms of TiN–TiB_2 ceramic at 400 °C. Mechanical polishing effect and removal of micro-fractured grains play important roles during room-temperature wear tests.

Keywords: A. Hot pressing; C. Friction; C. Wear resistance; D. Borides; D. Nitrides

1. Introduction

In recent years, a major challenge in advanced structural ceramics is to develop reproducible, long-lifetime ceramic sliding components for use in mechanical systems that involve high temperatures, heavy loads and high velocities. Refractory materials such as borides, nitrides and carbides are natural candidates for these tribological applications due to their exceptional hardness, wear resistance and thermal stability at high temperatures. Titanium diboride (TiB_2) is one kind of refractory compounds with high melting point, high elastic modulus, and high hardness. Titanium nitride (TiN) has some attractive properties, such as high hardness, good electrical conductivity and excellent wear resistance. However, both TiB_2 and TiN exhibit poor sinterability due to their high Peierls barriers to the dislocation movement, which restricts their industrial applications [1].

In combination the extreme resistance to plastic deformation of TiB_2 with the high–temperature plasticity of TiN, TiN–TiB_2 ceramics have attracted great attention on industrial applications as jet engine parts, armor plates, cutting tools, dies, and other high-temperature ceramic components [2,3]. TiN–TiB_2 ceramics were fabricated with self-propagating high-temperature synthesis (SHS) method using Ti (or TiH_2), B and BN powders as raw materials [4–6]. However, previous studies focused mainly on processing and microstructure; there is almost no report on mechanical and tribological properties of TiN–TB_2 ceramics in open literatures till now.

For brittle ceramics, the fracture toughness and hardness are two important factors for us to evaluate and understand their dry sliding wear behavior [7]. In the present paper, dense TiN–33.3 mol%TiB_2 ceramic was fabricated via the reactive hot-pressing process. Friction and wear properties of TiN–TiB_2 ceramic were then investigated in sliding against Al_2O_3 ball from room temperature to 700 °C in air to obtain a better understanding of wear mechanisms.

2. Experimental

In the present paper, commercial titanium (~30 μm, 99.9%) and hexagonal boron nitride powders (~150 nm, 99%) were used as the starting reactants in the reactive hot-pressing

* Corresponding author. Tel.: +86 451 86414291; fax: +86 451 86414291.
E-mail address: ouyangjh@hit.edu.cn (J.-H. Ouyang).

0272-8842/$36.00
doi:10.1016/j.ceramint.2010.05.019

process. The composition of reactive hot-pressed TiN–TiB_2 ceramic was designed according to a TiN/TiB_2 molar ratio of 2:1. The weighed powders were mixed by wet ball milling for 24 h in a polyethylene bottle with ZrO_2 balls and acetone as media. After mixing, the slurries were dried in a rotary vacuum evaporator, and then screened through a 120-mesh screen. The powder mixtures were heated to 1300 °C and held for 30 min, and then followed by hot pressing at 1800 °C for 1 h in vacuum with an applied pressure of 30 MPa. The bulk density of the specimens was measured by the Archimedes method, while the theoretical density was estimated by applying the rule of mixture. Specimens with dimensions of 3 mm × 4 mm × 36 mm were cut out from the sintered bodies using high-speed diamond cutter. These bars were ground with 1500-grit emery paper, and were finally polished with diamond slurries down to 1 μm finish. Three-point bending mode was used to measure flexural strength of samples over a span of 30 mm at a crosshead speed of 0.5 mm/min. Test pieces with the dimensions of 2 mm × 4 mm × 20 mm were prepared for measurements of single-edge notched beam (SENB) fracture toughness. Vickers hardness tests were carried out at a normal load of 98 N and room temperature. Each specimen was measured six times at selected load.

Friction and wear tests were conducted on a reciprocating ball-on-block high-temperature tribometer in sliding against sintered Al_2O_3 ball. The specimens with the dimensions of 4 mm × 8 mm × 16 mm were cut, ground and polished with emery papers and diamond slurries down to 1 μm finish. Before wear tests, polished specimens were ultrasonically cleaned first in acetone and then in ethanol. The test specimen was placed on a SUS310 stainless steel holder heated by a high-frequency induction heating coil. The paired Al_2O_3 ball, which is fixed on the upper holder in the tribo-tests, has a diameter of 9.5 mm and a Vickers hardness of 16 GPa. The displacement stroke, normal load, frequency, and testing time are the external variables associated with the tribometer. The wear tests were performed at loads of 5, 10 and 20 N, test temperatures of room temperature, 400 and 700 °C, a reciprocating frequency of 1 Hz, a linear stroke of 10 mm, and a test duration of 1200 s. The humidity during room-temperature wear tests is 40% in laboratory air. In addition, each specimen and its paired ball were heated from room temperature to testing temperature by high-frequency induction heating coil at a heating rate of 50 °C/min, and held at testing temperatures for 5 min before starting a new wear test. During the wear runs, the test temperature of the specimens was monitored using a thermocouple inserted at the near-surface position through a small hole in the SUS310 stainless steel holder. The friction coefficients were calculated by measuring the friction force at 1-ms intervals, obtaining the average friction force (absolute value) of one cycle of the reciprocation (1 s) and dividing the average friction force by the load.

Before and after wear tests, X-ray diffraction (XRD) analyses were conducted to determine the structure of reactive hot-pressed TiN–TiB_2 ceramic and to identify the possible structural changes of worn surfaces after wear tests at elevated temperatures. The XRD patterns were recorded using a Rigaku D/max 2550 diffractometer with a Cu Kα radiation. In order to estimate wear loss of the specimens after wear tests, the profilometry of worn surfaces were carried out by confocal laser scanning microscope (Olympus OLS3100, Japan). Morphologies of worn surfaces on each specimen were observed using a scanning electron microscope (FEI Quanta 200F, USA). The compositional analyses of worn surfaces were carried out using the energy dispersive spectroscopy (EDS) attachment. For SEM observations, the samples were coated with a thin Pt coating in order to obtain sufficient conductivity on the surface and avoid charging in the SEM.

3. Results and discussion

Fig. 1 shows the XRD pattern of reactive hot-pressed TiN–TiB_2 ceramic. The as-sintered sample consists only of TiN and TiB_2. Clearly, no residual BN and Ti from raw materials are detected. The reactive hot-pressed TiN–TiB_2 ceramic has a relative density of 98.6%, and exhibits excellent mechanical properties with a flexural strength of 731.9 MPa and a fracture toughness of 8.5 MPa $m^{1/2}$ at room temperature. As contrasted with the TiN–TiB_2 ceramics reported in previous studies [8,9], the reactive hot-pressed TiN–TiB_2 ceramic in present study shows remarkably high fracture toughness. The fracture toughness of TiN–TiB_2 ceramic obtained by Rangaraj et al. [8] via hot pressing the mixture of Ti and BN powders at 1850 °C is 6 MPa $m^{1/2}$, while the value obtained by Shobu et al. [9] via sintering the mixture of TiB_2 and TiN powders at 1900 °C is only 4 MPa $m^{1/2}$.

The backscattered electron image of reactive hot-pressed TiN–TiB_2 ceramic is shown in Fig. 2. The distribution of TiN (grey grains) and TiB_2 (dark grains) is very uniform. The average grain size of the TiN–TiB_2 ceramic is about 3 μm, which is smaller than that of monolithic TiB_2 hot pressed at 1800 °C for 1 h reported by Park et al. [10]. The fine microstructure and high flexure strength are closely related to the in situ synthesis of TiB_2 and TiN and mutual growth restriction of these two phases. Clearly, the fine microstructure and uniform distribution of TiB_2 and TiN phases are responsible for its high fracture toughness.

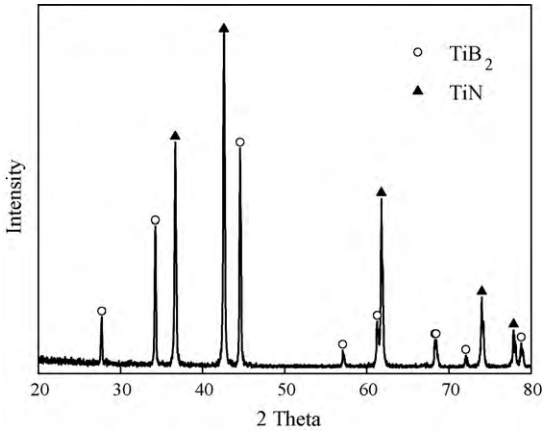

Fig. 1. XRD pattern of the reactive hot-pressed TiN–TiB_2 ceramic.

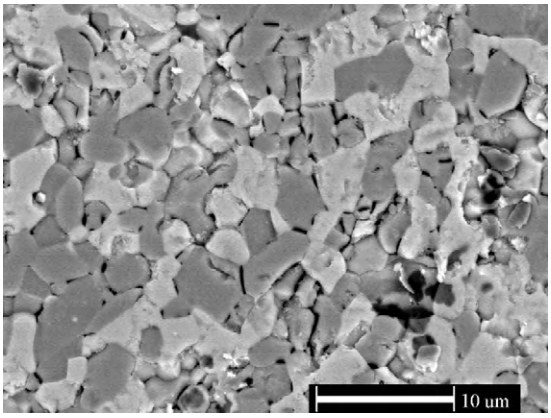

Fig. 2. Backscattered electron image of the reactive hot-pressed TiN–TiB_2 ceramic.

Fig. 3 shows the influence of temperature on friction coefficients of TiN–TiB_2 ceramic at 10 N load. The friction coefficients of TiN–TiB_2 ceramic at 700 °C are clearly lower than those obtained at room temperature and 400 °C. At 700 °C, friction coefficients of TiN–TiB_2 ceramic are relatively steady at the level of about 0.2 throughout the wear test. However, the friction coefficients obtained at 400 °C are much fluctuating during wear test. At room temperature, the friction coefficient exhibits an average value of 0.3 at the first 200 s, and decreases slowly at the following 150 s, and then remains an average value of 0.26 at the rest time.

The influence of load on friction coefficients of TiN–TiB_2 ceramic at elevated temperatures of 400 and 700 °C is shown in Fig. 4. At 700 °C, the friction coefficient exhibits a very slight decrease with the increase of load from 5 to 20 N. However, the situation is quite different at 400 °C with the increase of load. At 400 °C, the average friction coefficient is 0.4 at 5 N, 0.5 at 10 N and 0.68 at 20 N. Clearly, the friction coefficient of TiN–TiB_2 ceramic at 400 °C is closed related to the applied load. During wear test at 400 °C and 20 N load, an obvious decrease in friction coefficient is observed after a sliding time of 900 s. It is supposed to give information on the wear behavior of the debris or structural evolution at the interface. When the wear

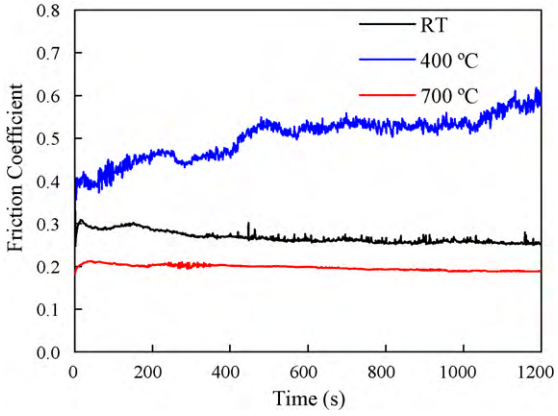

Fig. 3. Influence of temperature on friction coefficients of TiN–TiB_2 ceramic at 10 N load.

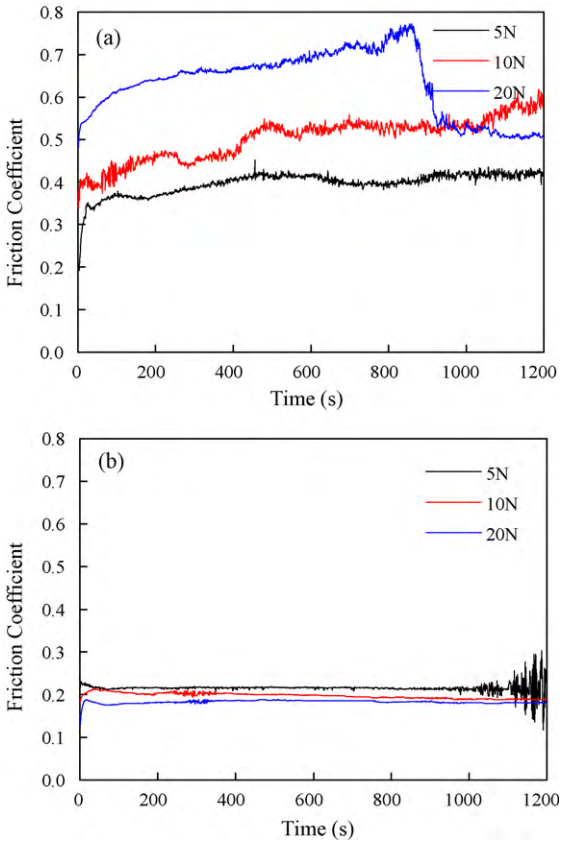

Fig. 4. Influence of load on friction coefficients of TiN–TiB_2 ceramic at different temperatures: (a) 400 °C; (b) 700 °C.

debris is removed from the interface or a certain lubricious interface forms, the friction coefficient will decreases [11,12].

In order to clarify the wear mechanisms of TiN–TiB_2 ceramic in sliding against alumina, the structural changes and morphologies of the worn surfaces after wear tests at different temperatures are investigated. Fig. 5 presents the XRD patterns of worn surfaces of TiN–TiB_2 ceramic after wear tests at 10 N and different temperatures. As contrasted with the XRD pattern of TiN–TiB_2 ceramic before wear tests (Fig. 1), no distinct difference is found on the worn surfaces of the TiN–TiB_2 specimens subjected to room temperature and 400 °C wear tests, however, a newly formed rutile (TiO_2) phase is clearly identified on the worn surface of the TiN–TiB_2 specimen subjected to 700 °C wear test. Monolithic TiN and TiB_2 begin to oxidize at around 500 and 400 °C respectively [13,14]. According to our previous studies on oxidation behavior of TiN–TiB_2, the following isothermal oxidation reactions take place at 700 °C:

$$TiN(s) + O_2(g) \rightarrow TiO_2(s) + (1/2)N_2(g) \quad (1)$$

$$TiB_2(s) + (5/2)O_2(g) \rightarrow TiO_2(s) + B_2O_3(l) \quad (2)$$

The oxidation of TiN–TiB_2 surface layer is believed to be a major reason for the sharp decrease in friction coefficient at 700 °C, which were reported in TiN or TiB_2-reinforced composites [15,16] and other non-oxide ceramics [12,17,18]. Under the elastically-loaded conditions in an elliptical contact, the

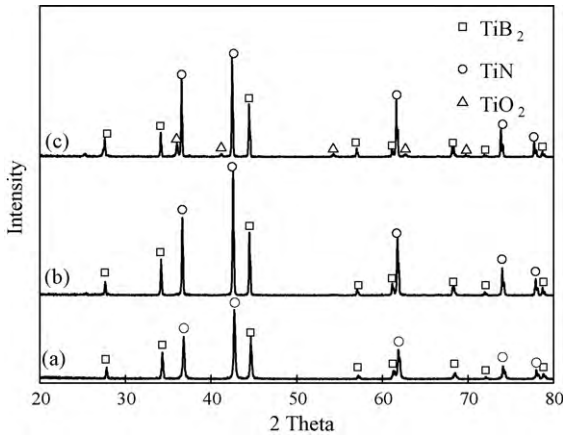

Fig. 5. XRD patterns of worn surfaces of TiN–TiB_2 ceramic after wear tests at different temperatures: (a) room temperature; (b) 400 °C; (c) 700 °C.

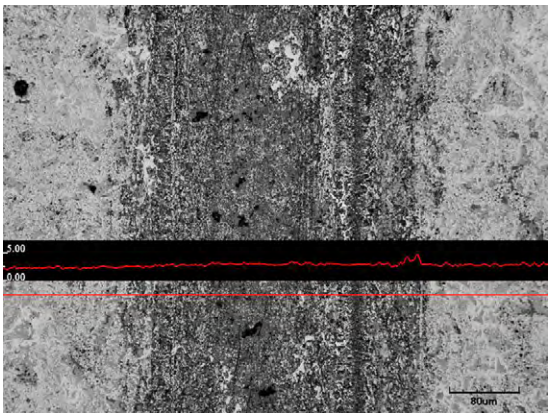

Fig. 6. Optical micrograph and two-dimensional profile of the wear track of TiN–TiB_2 after wear test at 400 °C.

lubrication fact of TiN–TiB_2 ceramic at 700 °C can be understood according to the following equation [19]:

$$\mu = A\frac{\tau}{P^{1/3}}\left[\frac{3}{4E'}\right]^{2/3} \quad (3)$$

where A is a constant determined by contact geometry, τ is critical shear stress at the interface, which may be an oxide film, P is the normal load, and E' is the effective elastic modulus of the contact materials. For a given contact geometry, friction coefficient is directly proportional to the critical shear stress. Rutile phase TiO_2 possesses a much lower critical shear stress than the substrate, which results in the reduced friction coefficient according to Eq. (3). As the area of the lubricious rutile film increases with increasing the applied load, the friction coefficient is inversely proportional to the applied load, which is consistent with the friction coefficient values of TiN–TiB_2 ceramic at 700 °C and different loads. It is concluded that the formation of lubricious rutile on the worn surface is the reason for the reduced friction coefficient when sliding in air at 700 °C.

In order to estimate the volume wear of TiN–TiB_2 ceramic after wear tests under different conditions, profilometry of the worn surfaces were conducted. All the specimens show a neglectable wear under different wear conditions in this investigation. A representative two-dimension profile of the wear track after wear test at 400 °C and 20 N load is presented in Fig. 6. As it is too difficult to distinguish the profile of the wear track, especially the wear depth is not measurable, it is impossible to calculate the wear rate by integration of the sectional worn area. The peak in the profile corresponding to the right edge of the wear track implies the accumulation of the debris.

A typical SEM micrograph of the worn surface of TiN–TiB_2 ceramic tested at room temperature and 10 N load is shown in Fig. 7. As presented in the region between the two red lines in Fig. 7(a), the wear track seem to be polished by the coupled alumina ball with very mild wear. However, propagation of cracks and spalling of fractured grains can be observed, as indicated in the magnified image of the wear track in Fig. 7(b). This suggests that the wear mechanism of TiN–TiB_2 wear at room temperature is mechanical polishing and micro-cracking, in which debris is mainly formed by the removal of micro-fractured grains.

Fig. 8 shows the micrographs of the worn surface of TiN–TiB_2 ceramic tested at 400 °C and 20 N load. As shown in Fig. 8(a), the worn surface appears to be covered with a thin smeared discontinuous tribofilm. Besides, pores and cracks, as marked in arrows in Fig. 8(a) and (b), are also observed in the wear track. These pores induced by the removal of fractured

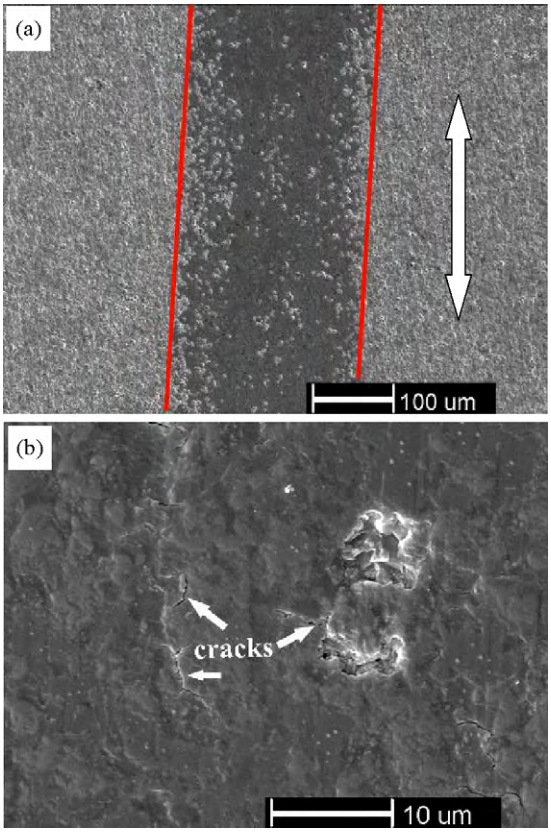

Fig. 7. Worn surface of TiN–TiB_2 ceramic tested at room temperature and 10 N load: (a) lower magnified SEM image of the worn surface; (b) higher magnified SEM image of the worn surface (double-headed arrow mark indicates the sliding direction).

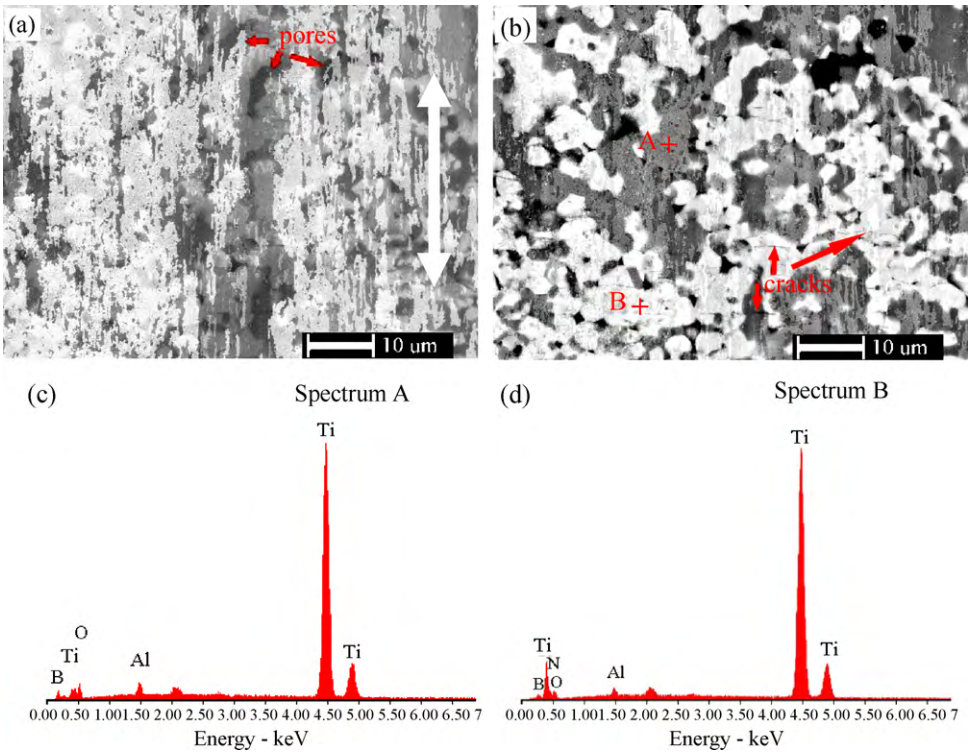

Fig. 8. Worn surface of TiN–TiB_2 ceramic tested at 400 °C and 20 N load: (a and b) secondary electron and backscattered electron images of the worn surface; (c and d) EDS spectra of different positions marked in (b) (double-headed arrow marks indicate the sliding direction).

grains verify that the initial wear is more related to the fractured debris. It is well known that cracks generated by Hertzian contact would be prone to propagate with the increase of normal load applied. The increase in friction coefficients of TiN–TiB_2 ceramic tested at 400 °C with increasing the applied load, as present in Fig. 4(a) would be expected. EDS analysis is conducted to identify the nature of the thin layer in Fig. 8(a). As shown in Fig. 8(c) and (d), Ti, B, N, O and Al elements are detected in the tribofilm, in which the former three elements are collected from the base TiN–TiB_2. According to the results of the EDS analysis, the proportion of O and Al elements were determined to be $>16\%$ and $<2\%$ respectively, which implies the tribooxides formed at 400 °C, presumably as a result of tribo-stressing and tribo-reaction at the contact areas.

Besides this widely covered tribo-oxidized film, dense alumina transferred layers were also observed at the edge of the wear track of TiN–TiB_2 ceramic sample. SEM observations and EDS analysis were conducted to identify this kind of alumina transferred layer, as presented in Fig. 9(a)–(c). Obviously, the transferred layer with a composition similar to alumna is different from the abovementioned tribo-oxidized film. In consideration of low fracture toughness and hardness of the coupled alumina ball as contrasted with the tested TiN–TiB_2 ceramic, alumina ball is prone to wear at 20 N load. These fractured wear particles are crushed to form fine wear debris during reciprocating motion. These transferred layers are supposed to generate from agglomeration of fine wear particles at the interface, and may form the compact surface layers. These compact transferred layers are effective in distributing contact stress and reducing wear.

In light of these results, what is occurring at 400 °C becomes clear. At 400 °C in dry air, the debris generated by intergranular fracture cause the increase of friction coefficient at the initial stage during wear test. With the increase of sliding time, tribo-oxidation products form and smear at the interface, and they will provide lubricity once they grow to a certain thickness and area. Meanwhile, the alumina wear debris would agglomerate to form dense transferred compacts to reduce wear.

The friction coefficients of TiN–TiB_2 ceramic in sliding against alumina ball at room temperature and 400 °C are discrepant. The friction coefficient obtained at room-temperature exhibits a relatively steady value around 0.3, whereas the frictional data obtained at 400 °C is fluctuating with a much higher value. This discrepancy is supposed to be related to different wear mechanisms of TiN–TiB_2 ceramic. Mild abrasive wear and tribo-oxidation wear are the dominant wear mechanisms of TiN–TiB_2 ceramic in sliding against alumina at 400 °C, however, mechanical polishing effects and removal of micro-fractured grains play important roles during room-temperature wear test.

As thermal oxidation occurs in the surface layer of the TiN–TiB_2 ceramic at 700 °C, the formation of lubricious oxidized products including solid rutile TiO_2 and liquid B_2O_3 at the tribo-contact regions will influence the friction and wear of TiN–TiB_2 ceramic. Fig. 10 shows the SEM micrograph and EDS analysis of worn surface of TiN–TiB_2 ceramic tested at 700 °C and 20 N load. The worn surface, as shown at the right side, is covered with continuous oxide film, however, dispersive TiO_2 rods can be found at the unworn region. No trace of glassy B_2O_3 layer is found on the surface. In consideration of the

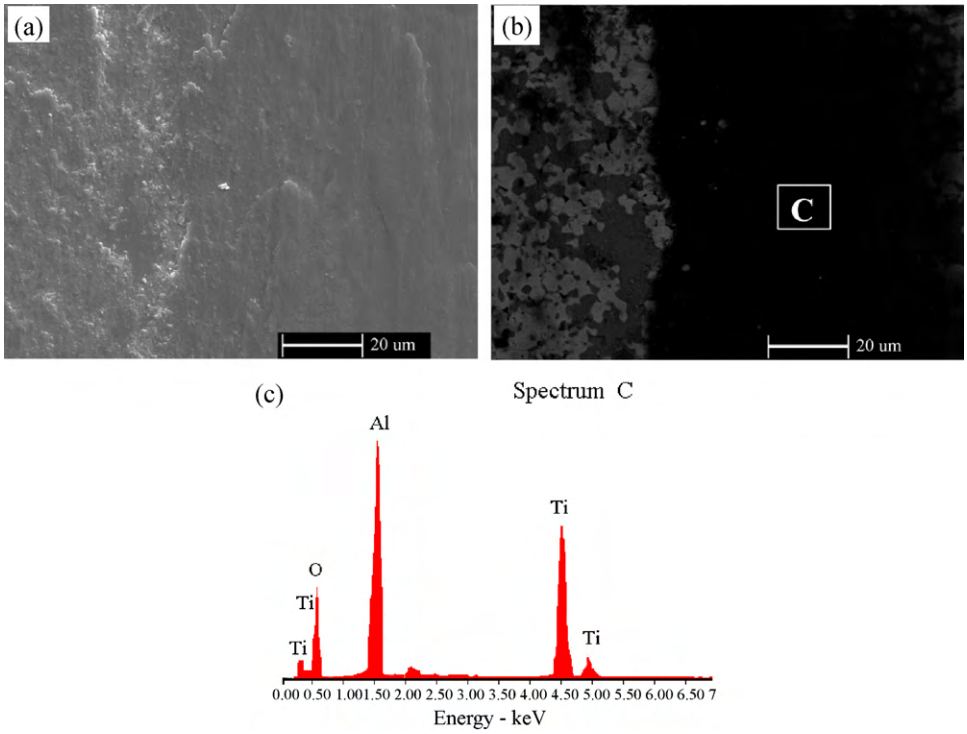

Fig. 9. SEM micrographs showing the alumina transferred layer formed on worn surface of TiN–TiB_2 ceramic tested at 400 °C and 20 N load: (a and b) secondary electron and backscattered electron images of the transferred layer; (c) EDS spectrum of the transferred layer.

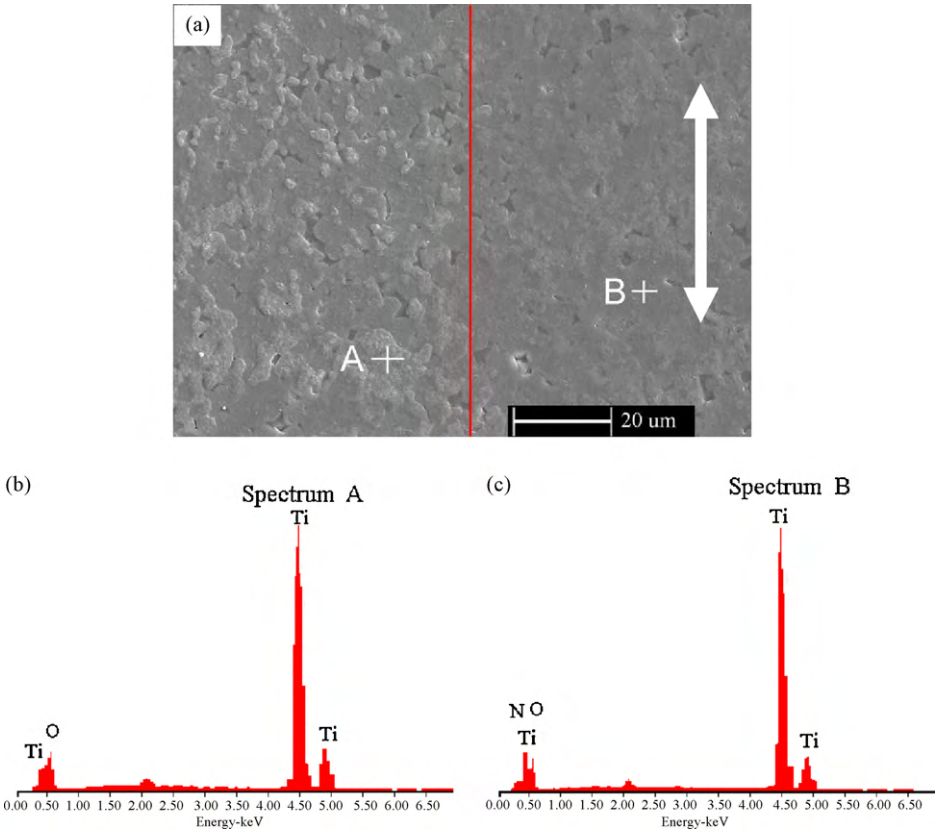

Fig. 10. Worn surface of TiN–TiB_2 ceramic tested at 700 °C and 20 N load: (a) SEM micrograph of the worn surface; (b and c) EDS spectra of different positions marked in (a) (double-headed arrow marks indicate the sliding direction).

relatively low melting temperature of B_2O_3 (450 °C) and the outward release of N_2 in Eq. (1), the B_2O_3 formed on the surface would evaporate intensely, which is consistent with the absence of B_2O_3 in the XRD and SEM analysis. Similar absence of B_2O_3 in oxidation of TiB_2 containing materials was also observed in the oxidation of TiB_2–$MoSi_2$ composites reported by Murthy et al. [20]. Therefore, the lubricious rutile phase generated on the worn surface due to thermal oxidation provides excellent lubrication effect at the tribo-contact regions and greatly reduce the friction coefficient of TiN–TiB_2 ceramic at 700 °C.

4. Conclusions

The reactive hot-pressed TiN–TiB_2 ceramic has a distinctly different friction characteristic in sliding against alumina ball at room temperature, 400 °C and 700 °C. The TiN–TiB_2 ceramic exhibits a distinct decrease in friction coefficient at 700 °C as contrasted with the friction data obtained at room temperature and 400 °C.

Wear mechanisms of TiN–TiB_2 ceramic depend mainly upon testing temperature at identical applied loads. Lubricious oxidized products caused by thermal oxidation provide excellent lubrication effects and greatly reduce the friction coefficient of TiN–TiB_2 ceramic at 700 °C. However, mild abrasive wear and tribo-oxidation are the dominant wear mechanisms of TiN–TiB_2 ceramic at 400 °C. Mechanical polishing effects and removal of micro-fractured grains play important roles during room-temperature wear test.

Acknowledgments

The authors would like to thank financial supports from the National Natural Science Foundation of China (NSFC-No. 50572020), the National 863 High-Tech Project (2006AA03Z537), and the Program for New Century Excellent Talents in University (NCET-06-0339).

References

[1] J.R. Ramberg, C.F. Wolfe, W.S. Williams, Resistance of titanium diboride to high-temperature plastic yielding, J. Am. Ceram. Soc. 68 (1985) 78–79.
[2] M.W. Barsoum, B. Houng, Transient plastic phase processing of titanium–boron–carbon composites, J. Am. Ceram. Soc. 76 (1993) 1445–1451.
[3] D. Brodkin, S.R. Kalidindi, M.W. Barsoum, A. Zavaliangos, Microstructural evolution during transient plastic phase processing of titanium carbide–titanium boride composites, J. Am. Ceram. Soc. 79 (1996) 1945–1952.
[4] C.L. Yeh, G.S. Teng, Combustion synthesis of TiN–TiB_2 composites in Ti/BN/N_2 and Ti/BN/B reaction systems, J. Alloys Compd. 424 (2006) 152–158.
[5] R. Tomoshige, A. Murayama, T. Matsushita, Production of TiB_2–TiN composites by combustion synthesis and their properties, J. Am. Ceram. Soc. 80 (1997) 761–764.
[6] J.W. Lee, Z.A. Munir, Synthesis of dense TiB_2–TiN nanocrystalline composites through mechanical and field activation, J. Am. Ceram. Soc. 84 (2001) 1209–1216.
[7] T.E. Fischer, Z. Zhu, H. Kim, D.S. Shin, Genesis and role of wear debris in sliding wear of ceramics, Wear 245 (2000) 53–60.
[8] L. Rangaraj, C. Divakar, Reactive hot pressing of titanium nitride–titanium diboride composites at moderate pressures and temperatures, J. Am. Cerm. Soc. 87 (2004) 1872–1878.
[9] K. Shobu, T. Watanabe, Frictional properties of sintered TiN–TiB_2 and Ti(CN)–TiB_2 ceramics at high temperature, J. Am. Ceram. Soc. 70 (1987) C-103–C-104.
[10] J.-H. Park, Y.-H. Koh, H.-E. Kim, C.S. Hwang, E.S. Kang, Densification and mechanical properties of titanium diboride with silicon nitride as a sintering aid, J. Am. Ceram. Soc. 82 (1999) 3037–3042.
[11] J. Denape, J. Lamon, Sliding friction of ceramics: mechanical action of the wear debris, J. Mater. Sci. 14 (1990) 114–116.
[12] C. Blanc, F. Thebenot, D. Treheux, Wear resistance of αSiC-TiB_2 composites prepared by reactive sintering, J. Eur. Ceram. Soc. 19 (1999) 571–579.
[13] H.-Y. Chen, Oxidation behavior of titanium nitride films, J. Vac. Sci. Technol. 23 (2005) 1006–1009.
[14] A. Tampieri, A. Bellosi, Oxidation of monolithic TiB_2 and of Al_2O_3–TiB_2 composite, J. Mater. Sci. 28 (1993) 649–653.
[15] N. Fateh, G.A. Fontalvo, G. Gassner, C. Mitterer, Influence of high-temperature oxide formation on the tribological behavior of TiN and VN coatings, Wear 262 (2007) 1152–1158.
[16] T. Senda, Y. Yamamoto, Y. Ochi, Friction and wear test of titanium boride ceramics at elevated temperatures, J. Ceram. Soc. Jpn. 101 (1993) 461–465.
[17] O.O. Ajayi, A. Erdemir, R.H. Lee, F.A. Nichols, Sliding wear of silicon carbide–titanium diboride ceramic–matrix composite, J. Am. Ceram. Soc. 76 (1993) 511–517.
[18] S. Gupta, D. Filimonov, V. Zaitsev, T. Palanisamy, M.W. Barsoum, Ambient and 550 °C tribological behavior of select MAX phases against Ni-based superalloys, Wear 264 (2008) 270–278.
[19] H.Y. Liu, M.E. Fine, H.S. Cheng, A.L. Geiger, Lubricated rolling and sliding wear of SiC_W/Si_3N_4 composite against M2 tool steel, J. Am. Ceram. Soc. 76 (1993) 105–112.
[20] T.S.R.Ch. Murthy, R. Balasubramaniam, B. Basu, A.K. Suri, M.N. Mungol, Oxidation of monolithic TiB_2 and TiB_2–20 wt.% $MoSi_2$ composite at 850 °C, J. Eur. Ceram. Soc. 26 (2006) 187–192.